

# REPORT DOCUMENTATION PAGE

AFRL-SR-BL-TR-99-

0281

Public reporting burden for this collection of information is estimated to average 1 hour per response, including the time for reviewing the collection of information. Send comments regarding this burden estimate or any other aspect of this collection of information Operations and Reports, 1215 Jefferson Davis Highway, Suite 1204, Arlington, VA 22202-4302, and to the Office of Management or

completing and reviewing  
factorate for information

1. AGENCY USE ONLY (Leave blank)

2. REPORT DATE

01 Feb 98 to 30 Apr 99 Final

4. TITLE AND SUBTITLE

Nonlinear Spatio-Temporal processing of femtosecond pulses for ultrahigh bandwidth communication

5. FUNDING NUMBERS

62173C  
1651/05

6. AUTHOR(S)

Professor Fainman

7. PERFORMING ORGANIZATION NAME(S) AND ADDRESS(ES)

University of California, San Diego  
9500 Gilman Drive  
La Jolla, CA 92093-0934

8. PERFORMING ORGANIZATION  
REPORT NUMBER

9. SPONSORING/MONITORING AGENCY NAME(S) AND ADDRESS(ES)

AFOSR/NE  
801 North Randolph Street Rm 732  
Arlington, VA 22203-1977

10. SPONSORING/MONITORING  
AGENCY REPORT NUMBER

F49620-98-1-0266

11. SUPPLEMENTARY NOTES

12a. DISTRIBUTION AVAILABILITY STATEMENT

APPROVAL FOR PUBLIC RELEASE; DISTRIBUTION UNLIMITED

12b. DISTRIBUTION CODE

13. ABSTRACT (Maximum 200 words)

We emphasize developing high speed and high efficiency parallel-to-serial multiplexers and serial-to-parallel demultiplexers, the two most critical challenges for current technology to meet the needs of ultra-high bandwidth communication applications. In the following we describe research on nonlinear spatio-temporal processors using cascaded second order nonlinearity to perform (A) Spatial-temporal wave mixing for space-to-time conversion, and (B) Instantaneous time-reversal and phase-conjugation of ultrafast waveforms. In addition, we will also report our study on a (C) Femtosecond single-shot pulse imaging system that uses transverse-time-delay pulse cross-correlation.

14. SUBJECT TERMS

19991208 204

15. NUMBER OF PAGES

16. PRICE CODE

17. SECURITY CLASSIFICATION  
OF REPORT

UNCLASSIFIED

18. SECURITY CLASSIFICATION  
OF THIS PAGE

UNCLASSIFIED

19. SECURITY CLASSIFICATION  
OF ABSTRACT

UNCLASSIFIED

20. LIMITATION OF  
ABSTRACT

UL

DTIC QUALITY INSPECTED 4

Standard Form 298 (Rev. 2-89) (EG)  
Prescribed by ANSI Std. Z39.18  
Designed using Perform Pro, WHS/DIOR, Oct 94

UNIVERSITY OF CALIFORNIA, SAN DIEGO

BERKELEY • DAVIS • IRVINE • LOS ANGELES • RIVERSIDE • SAN DIEGO • SAN FRANCISCO



SANTA BARBARA • SANTA CRUZ

DEPARTMENT OF ELECTRICAL AND COMPUTER ENGINEERING  
9500 GILMAN DRIVE

LA JOLLA, CALIFORNIA 92093-0407

Prof. Y. Fainman

Ph: (619) 534-8909

Fax: (619) 534-1225

E-mail: fainman@ece.ucsd.edu

September 14, 1999

Dr. Kent Miller  
AFOSR/NE  
801 North Randolph Street, Room 732  
Arlington, VA 22203-1977

Dear Dr. Miller:

Please find enclosed the final technical report for the grant F-49620-98-10-0266 entitled "Nonlinear spatio-temporal processing of femtosecond pulses for ultrahigh bandwidth communication."

Should you have any questions about this report, please do not hesitate to contact me.

Sincerely,

A handwritten signature in cursive script, appearing to read "Shaya".

Y. Fainman

Professor

Final Technical Report

for AFOSR

**Nonlinear spatio-temporal processing of femtosecond pulses  
for ultrahigh bandwidth communication**

Sponsored by

**Air Force Office of Scientific Research**

and

**Ballistic Missile Defence Organization**

Under Grant F49620-98-10-0266

for Period 2/1/98 through 9/30/99

total: \$225,000

Grantee

The Regents of the University of California, San Diego

University of California, San Diego

La Jolla, CA 92093

**Principal Investigators:**

Y. Fainman  
(619) 534-8909

P.-C. Sun  
(619) 534-7891

**Program Manager:**

Dr. K. Miller and A. Craig,  
(703) 696-8573

Dr. L. Lome  
(703) 588-7416

## **2. Objectives/Statement of work**

- A. Study of the nonlinear spatio-temporal processing technology to achieve real-time optical space-time signal processing for ultrahigh bandwidth communication.
- B. Study of high-speed pulse detection with transverse-time-delay pulse cross-correlation technique.

## **3. Status of effort**

We have developed a nonlinear optical spatio-temporal processor that allows one to perform real-time optical information processing in both space-domain and time-domain. The nonlinear optical processor is based on a Cascaded Second-order Nonlinearity (CSN) to achieve efficient four-way mixing of signals carried by optical fields. Theoretical and experimental results, such as real-time space-to-time conversion and real-time optical time reversal and temporal phase conjugation have been demonstrated. We have also developed a pulse imaging technique based on the transverse-time-delay pulse cross-correlation technique.

## **4. Accomplishments/New Findings**

We emphasize developing high speed and high efficiency parallel-to-serial multiplexers and serial-to-parallel demultiplexers, the two most critical challenges for current technology to meet the needs of ultra-high bandwidth communication applications. In the following we describe research on nonlinear spatio-temporal processors using cascaded second order nonlinearity to perform (A) Spatial-temporal wave mixing for space-to-time conversion, and (B) Instantaneous time-reversal and phase-conjugation of ultrafast waveforms. In addition, we will also report our study on a (C) Femtosecond single-shot pulse imaging system that uses transverse-time-delay pulse cross-correlation.

### **A. Spatial-temporal wave mixing for space-to-time conversion**

We report the first successful realization of a real-time space-to-time conversion technique capable of generating synthesized temporal waveforms at the output, controlled by a spatial domain image with a femtosecond response time and high conversion efficiency. The nonlinear process, based on a cascaded second-order nonlinearity (CSN) arrangement, consists of a frequency-up process followed by a frequency-down process satisfying the type-II non-collinear phase matching condition. The non-linear wave mixing in our experiment takes place in the Fourier domain of the temporal and spatial channels (see Fig. 1). The first nonlinear process of the cascade mixes the Spectral Decomposition Wave (SDW) field  $U_1$  of an ultrashort input pulse, with the spatial Fourier Transform (FT) field  $U_2$  of a quasi-monochromatic wave spatially modulated by a one-dimensional image. The fields  $U_1$  and  $U_2$  are polarized in the ordinary and extraordinary direction, respectively, relative to the optical axis of the nonlinear crystal and their propagation directions satisfy the phase matching condition. The waves  $U_1$  and  $U_2$  generate the intermediate up-converted wave  $U_{int} \sim \chi^{(2)} U_1 U_2$ , oscillating at the sum frequency, propagating along the optical axis of the setup, and polarized in the extraordinary direction. The second nonlinear process of the cascade mixes the intermediate wave  $U_{int}$  and the spatial FT of a narrow slit (implementing a one-dimensional spatial Dirac  $\delta$ -function),  $U_3$ . The narrow slit in the second spatial channel is illuminated by the same quasi-monochromatic source as  $U_2$ , and co-propagates with  $U_2$  after a polarizing beam splitter (see Fig. 1). The wave  $U_3$  is polarized in the ordinary direction and interacts with the extraordinary polarized intermediate wave  $U_{int}$ . Since  $U_3$  contains no information in either the space or the time domain, its function is to down-convert the carrier frequency of the complex field of  $U_{int}$ . In this arrangement, the phase matching condition for the down-conversion process is automatically satisfied. The resultant wave,  $U_4 \sim \chi^{(2)} U_{int} U_3^*$ , propagates in the same directions as  $U_1$  and at the same center frequency but in an orthogonal polarization state. The resultant wave is therefore proportional to the input waves as

$U_4 \sim (\chi^{(2)})^2 U_1 U_2 U_3^*$ , which is equivalent to a four-wave mixing process. When comparing the expression for the resultant wave to the SDW of the input temporal channel, we can observe that the spatially dispersed frequency components are modulated by the information of the spatial mask. Thus, the femtosecond rate spatial-temporal processing has generated the SDW of the output temporal optical waveform. The SDW  $U_4$  is recombined in the optical setup by a second FT lens and grating diffraction to yield the output temporal signal. This synthesized waveform is a convolution of the input ultrashort pulse with a space domain image, whose spatial dependence has been converted to temporal dependence in the spatial-temporal processor. When the duration of the ultrashort pulse is much shorter than the feature size of the temporally mapped mask, then  $p(t)$  can be approximated by a Dirac  $\delta$ -function and the output temporal waveform is directly proportional to the information in the mask.

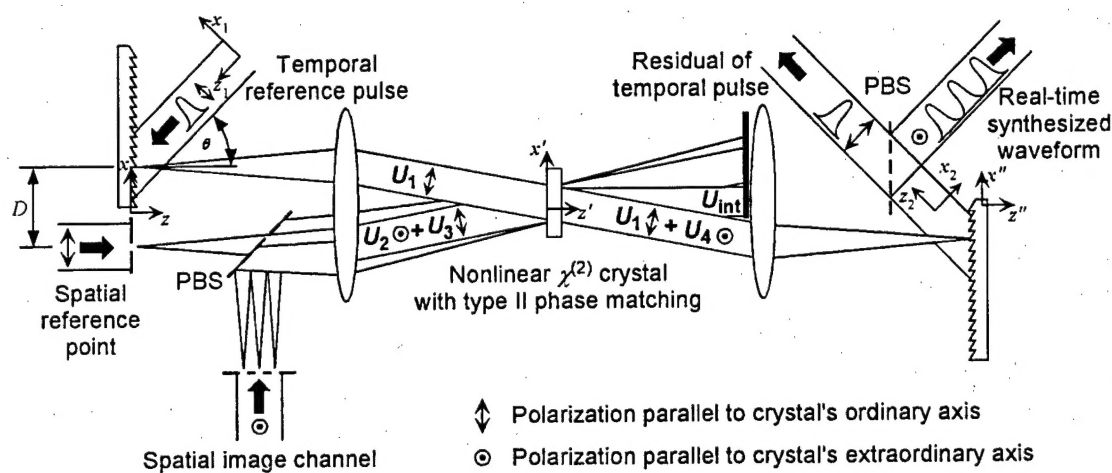


Fig. 1 Experimental setup of the spatial-temporal processor. The CSN enables time-space information exchange via a four-wave mixing process.

We demonstrate experimentally the CSN spatial-temporal wave mixing using ultrashort pulses of 100 fs duration at a center wavelength of 800 nm with an energy level of 1 mJ per pulse (generated from a Ti:Sapphire ultrashort pulse oscillator combined with a regenerative amplifier). Ten percent of the power of the laser pulse is split off and introduced into the temporal input channel of the processor, generating the SDW  $U_1$ . The SDW is generated by a 600 lines/mm blazed grating and a lens of 375 mm focal length. The remaining 90% of the pulse power is used to generate the light source for the implementation of the spatial channels by stretching the pulse width with a grating pair to a several picosecond duration (i.e., chirped pulse), matching the time window of the temporal channel. The stretched pulse is divided into the two spatial channels for implementing waves  $U_2$  and  $U_3$ . Since the CSN process occurs with femtosecond-scale time response due to the fast nonlinearity, a sufficient condition for the four-wave mixing operation is for the two spatial channels to be instantaneously equal. The spatial-temporal wave mixing by the  $\chi^{(2)}$  media is performed in a 2-mm thick type II  $\beta$ -barium borate (BBO) crystal. In our experiment, the entire process is derived from a single pulse from the laser source; thus, the information exchange is done on a single-shot basis. The maximum conversion efficiency of the input SDW  $U_1$  to the filtered output SDW  $U_4$  is 10%, limited by fundamental wave depletion. The high conversion efficiency illustrates the advantage of the CSN approach as opposed to conventional  $\chi^{(3)}$  nonlinearity for four-wave mixing.

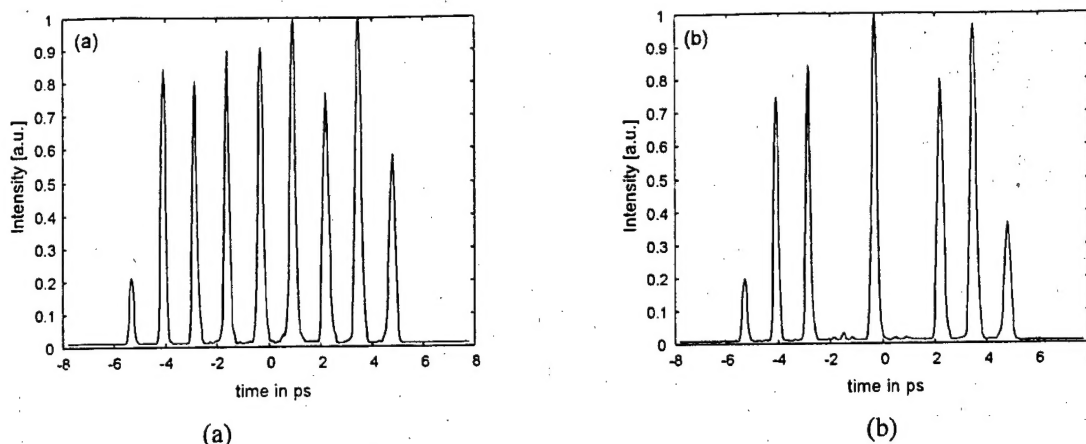


Fig. 2 Synthesized temporal waveform generated by a spatial information mask consisting of a sequence of equally spaced point sources. (a) All point illuminated by quasi-monochromatic light. (b) Two point sources blocked.

In our first spatial-temporal information transfer experiment, we use a mask containing a sequence of narrow slits spaced 0.8 mm apart. To achieve high light throughput, the illuminating beam is focused into the slits with a cylindrical lenslet array. The shaped waveform, consisting of a sequence of pulses, is observed with a real-time pulse imaging technique (see Fig. 2). As predicted, the synthesized waveform consists of a sequence of pulses separated by  $\sim 1.3$  ps (mapping spatial separation of 0.8 mm to time). Selectively blocking some of the slits results in a matching temporal waveform, confirming our ability to perform single-shot temporal waveform synthesis in real-time from a spatial channel. These results are generated under maximal conversion efficiency, where a fundamental wave depletion is observed. Therefore, by blocking some of the slits, more photons are upconverted by the spatial waves of the open slits, leading to an amplitude distribution change in the pulse sequences of Fig. 2. No evidence of crosstalk between the channels is detected.

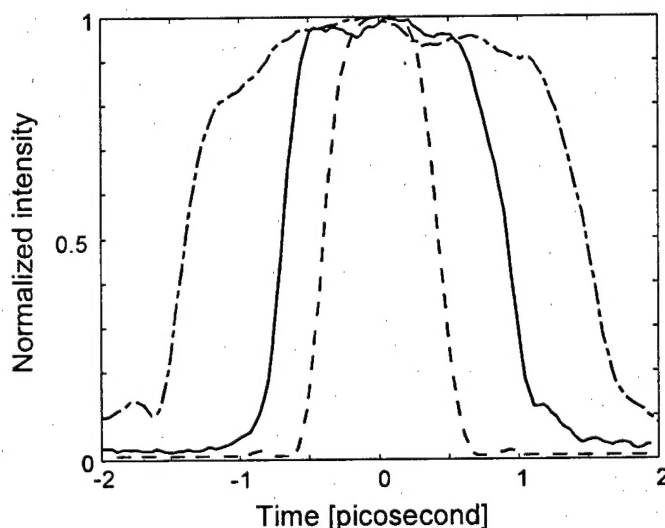


Fig. 3 Superimposed images of square pulses generated by a varying the width of a square aperture in the spatial channel.

Generation of synthesized square pulses by spectral filtering is not a simple task. The mask should contain amplitude information over a wide dynamic range as well as phase information for implementing negative values. Space-to-time mapping techniques simplify the task of complex mask preparation, while the requirement for a wide dynamic range in the



recording medium remains. In our wave-mixing approach with CSN, the amplitude of the synthesized wave is dependent upon the amplitudes of the three input waves (as long as wave depletion and phase mismatch are negligible). This linear relationship gives rise to high-fidelity conversion from space-to-time. An adjustable slit is placed in the spatial information channel to experiment with several synthesized square pulse durations. The generated waveforms are modified in real-time by changing the slit width, and the square pulses are immediately observed with the pulse imager on a monitor. At wide slit widths, non-uniformity across the top of the square pulse is observed (see Fig.3). We have verified that the reason is due to non-uniformity in the illumination of the spatial channel. An image of the spatial information channel in the space-to-time processor matches well with the observed image of the synthesized waveform in the time-to-space converter.

To demonstrate the ability to encode phase information, a point source, generated by focusing the spatial beam with a cylindrical lens, is used as the spatial information channel. Translating the lens longitudinally away from the input plane forms a spherical wavefront with variable quadratic phase on the input plane of the spatial information channel. As the translation of the line source from the input plane is increased (in either the positive or the negative direction), the output SDW acquires a larger positive or negative quadratic phase and after recomposing on the output grating, emerges as a chirped pulse (either a positive or negative chirp). The measured synthesized chirped pulses exhibit, as expected, broader pulses along with a reduction of the peak intensity (see Fig. 4a). We estimate the amount of chirp using the pulse imager and as expected we find direct correspondence between the longitudinal translation of the focusing lens and the amount of chirp on the synthesized waveform. We have verified experimentally the relation by finding the location where the output of the pulse imager focuses, for each translated location used in the spatial channel of the space-to-time converter (see Fig. 4b). Thus, we have a correspondence between the longitudinal translation of the line source in the input spatial channel of the spatial-temporal processor and the longitudinal translation of the focus plane of the pulse imager.

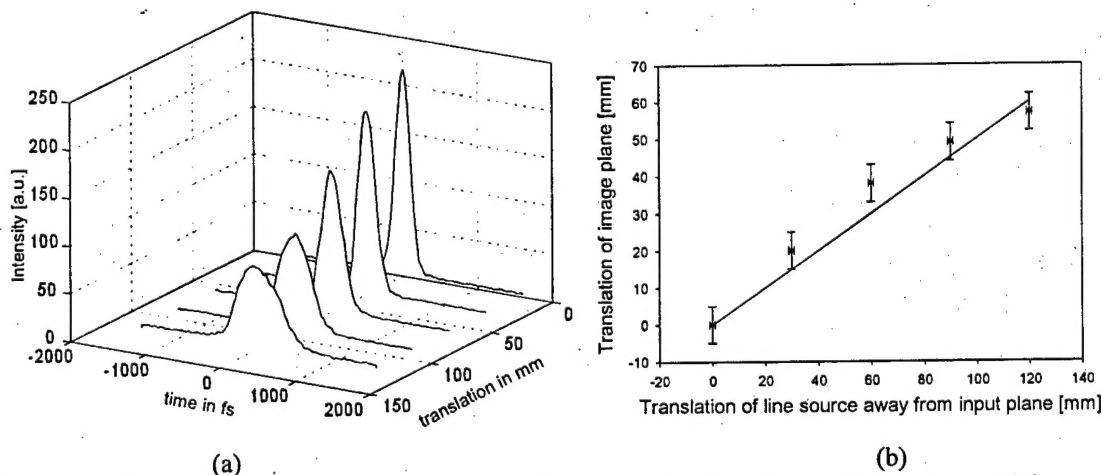


Fig. 4 (a) Synthesized temporal waveforms generated by a quadratic wave front in the spatial channel, generating chirped pulses. Quadratic wave front generated by longitudinally translating a point source from the input plane. (b) Linear correspondence between translation of point source away from input plane of space-to-time converter and translation of image formation plane in the pulse imager. Solid line corresponds to theoretical curve of slope 1/2.

Relative to other spatial-temporal processing techniques, the CSN approach provides femtosecond rate processing due to the fast bound electron nonlinearity and high efficiency on account of a relatively large  $\chi^{(2)}$  coefficient. The spatial-temporal process that we have demonstrated generates an output temporal waveform that can be reconfigured in real time and is proportional to the convolution of an input ultrashort pulse and a spatial image. Furthermore,

wavelength tuning of the synthesized temporal waveform can be achieved by using different temporal frequencies in the two spatial channels (with a correction to the propagation direction, to satisfy phase matching). For operation with pulsed lasers at high repetition rates, the spatial channels may be implemented by a second intense CW laser source, or, the conversion efficiency of the CSN process should be improved. Since the technique realizes a general four-wave mixing process of temporal and spatial information-carrying waves, the setup may be converted to provide the convolution or correlation signal between spatial and temporal channels, with the output in either the temporal or the spatial domain. Thus, this spatial-temporal process can be considered a fundamental system for performing ultrafast signal processing on optical waveforms in the time and space domain.

## B. Instantaneous time-reversal and phase-conjugation of ultrafast waveform

We report the generation of a true time-reversed waveform for complex amplitude ultrafast waveforms, by inverting the spectral information of the signal about the center frequency. We perform the two time reversal techniques—conventional spectral phase conjugation and the novel spectral information inversion—by wave mixing four spectrally decomposed waves utilizing a cascaded process in a  $\chi^{(2)}$  nonlinear crystal. The unique attributes of our approach include instantaneous (femtosecond-scale) response time, high conversion efficiency and a long time-window.

In contrast to the previously demonstrated spatial-temporal processor, the arrangement in this experiment consists of wave-mixing spectrally decomposed waves (SDW). We introduce three ultrafast waveforms to the spectral processing device (SPD): a complex amplitude temporal information waveform and two transform-limited ultrashort pulses, to serve as reference pulses (see Fig. 5). In the spectral inversion arrangement case, the spectral decompositions of the ultrafast waveforms are spatially dispersed in opposite directions by diffracting from a grating +1 and -1 orders at the SPD's input.

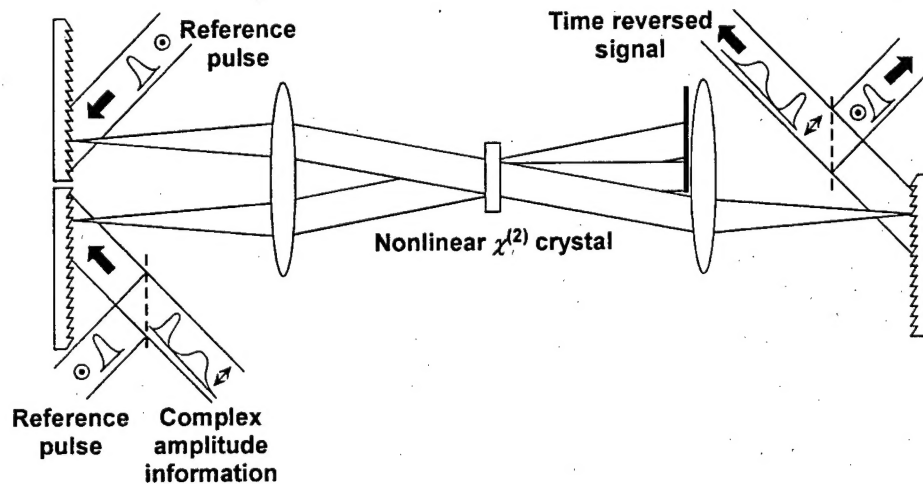


Fig. 5 Experimental setup for true time reversal: Nonlinear four wave mixing of mutually inverted spectrally decomposed waves by CSN results in instantaneous time reversal of complex amplitude ultrafast waveforms. PBS, polarizing beam splitter

The spectrum of the wave  $U_2$  is inverted with respect to the spectra of  $U_1$  and  $U_3$  due to the opposite directions of spatial dispersion corresponding to the +1 and -1 diffraction orders. The frequency-sum process mixes the SDW  $U_1$  and  $U_2$ , generating the intermediate wave  $U_{int} = \chi^{(2)} U_1 U_2$ . Due to the energy conservation principle, the intermediate wave is quasi-monochromatic at every spatial location  $x'$ . The spectral information from the input temporal



signal is preserved in the wave mixing process, and is converted to spatial modulation of the intermediate wave. These two desirable properties were used in the past to perform ultrafast waveform imaging. The second nonlinearity in the cascade is a frequency-difference process that mixes  $U_{int}$  with the SDW of  $U_3$ , generating an output SDW  $U_4 = \chi^{(2)} U_{int} U_3^*$ . The spectral information in  $S(\bullet)$  is inverted with respect to the spatial dispersion direction, thus achieving our goal of spectral information inversion. The SDW  $U_4$  is recomposed by the second grating of the SPD to yield the output temporal waveform  $y(t) = s(-t) \otimes r(t) \otimes r^*(t)$ , where  $\otimes$  denotes the convolution operator. As  $r(t)$  is a transform limited reference pulse, the conjugation term on the last expression may be dropped. The generated output signal is therefore proportional to the time-reversed signal waveform convolved twice with a reference pulse, broadening the temporal features of the signal waveform. The processor's time window can be tailored to the desired application, usually in the several picosecond range.

Our second time reversal experiment is based on generating the phase conjugate of the signal spectrum, useful for time reversal of real amplitude waveforms as well as dispersion compensation in transmission links. The arrangement of Fig. 1 is modified such that the three waves enter the SPD from the same direction, utilizing the same diffraction order, and the signal information wave is used to instigate the down-conversion process. We find that the output temporal waveform in this case is  $\hat{y}(t) = s^*(-t) \otimes r(t) \otimes r(t)$ . The only difference in the two resulting time reversed waveforms,  $\hat{y}(t)$  and  $y(t)$ , is the conjugation operation on the signal waveform. If one constrains the information signals to contain only real data, the time reversal and the phase-conjugate results are equivalent. For complex amplitude information, the two results will differ.

Both time reversal experiments were performed in a SPD consisting of 600 line/mm blazed gratings and lenses of 375 mm focal length, with a 2-mm long  $\beta$ -barium borate (BBO) crystal placed in the Fourier plane. The three input waveforms were derived from a single ultrashort pulse (generated from a Ti:sapphire ultrashort pulse oscillator combined with a regenerative amplifier) with 100 fsec duration, center wavelength of 800 nm, and energy level <1 mJ. The signal waveform contained 10% of the optical power and the remaining 90% were used for the reference pulses (which serve as pump waves), to maximize the conversion efficiency. To demonstrate the true time reversal property of complex amplitude waveforms by wave mixing oppositely dispersed SDW's, we used a complex waveform signal consisting of a transform limited pulse followed by a positively chirped pulse. The waveform was generated by an unequal arm Mach-Zender interferometer with a grating pair placed in one arm. The input information signal,  $s(t)$ , and the two time-reversed waveforms,  $y(t)$  and  $\hat{y}(t)$ , were analyzed by a real-time ultrafast waveform imaging system, which has the following desirable property: the quadratic phase—mapped onto the spatial domain—is compensated by free space propagation, i.e., by displacing the output detection plane of the imager. In this manner, the magnitude and sign of the quadratic phase term of the ultrafast waveform that is imaged can be measured.

Figure 6 shows the experimental results of ultrafast waveform imaging for the input information signal,  $s(t)$ , and the two time-reversed waveforms,  $y(t)$  and  $\hat{y}(t)$ , illustrating the difference between the two techniques of generating time reversed waveforms. The input temporal signal consists of a transform limited pulse followed by the chirped pulse (see Fig. 6-(a)). By displacing the observation plane closer to the Fourier transform lens, the quadratic phase is canceled and the chirped pulse is focused to its tightest spot (see Fig. 6-(d)). Both time reversal methods exchanged the location of the two pulses (see Figs. 6 (b)-(c)). The true time reversal experiment preserved the quadratic phase sign information, as evident by the chirped pulse focusing closer to the lens (see Fig. 6-(e)), whereas the phase conjugate signal reversed the sign of the quadratic phase (see Fig. 6-(f)). Wave mixing mutually inverted SDW's has the additional benefit of better phase matching in the wave-mixing process for different temporal frequency components, as group velocity mismatch is spatially compensated.<sup>10</sup> Therefore, the

true time reversed signal supported a broader bandwidth, resulting in higher resolution spatial images (compare the relative widths of the transform limited pulse and the chirped pulse in the true time reversal and phase conjugation cases). The conversion efficiency of the wave mixing process was 14%, defined by the ratio of the powers of the time-reversed waveform to that of the input signal waveform. The high conversion efficiency is attributed to the effective energy transfer of the CSN process.

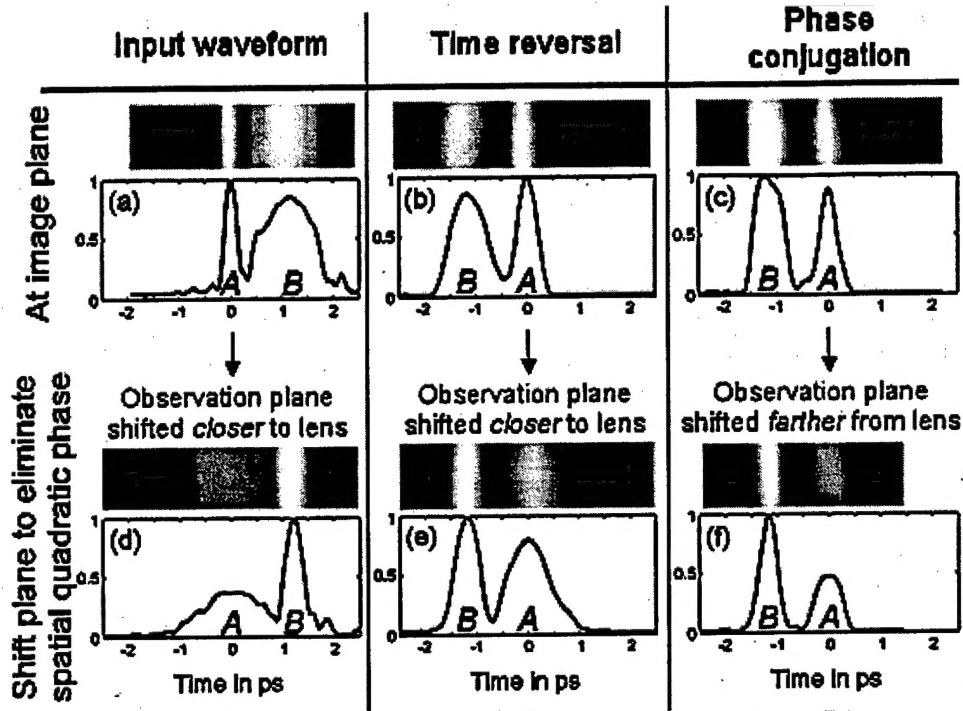


Fig. 6 Spatial images of ultrafast waveforms in the time reversal experiments: (a) input signal, and time reversed signals by (b) spectral inversion and (c) phase conjugation. Input pulses, A and B, are transform limited and positively chirped, respectively. Both methods of time reversal exchange the location of the pulses, but the true time reversal preserves the complex amplitude information, as determined by the quadratic phase of pulse B. Displacing the image plane closer [in (d) and (e)] or farther [case (f)] to lens compensates for positive or negative quadratic phase, respectively. Detected CCD images of the ultrafast waveforms are shown as well as the extracted temporal information.

### C. Femtosecond Single Shot Correlation System: A time domain approach

We introduce, analyze and experimentally demonstrate a new pulse correlation technique that is capable of real-time conversion of a femtosecond pulse sequence into its spatial image. Our technique uses a grating at the entrance of the system, introducing a Transverse-Time-Delay (TTD) into the transform limited reference pulse. The shaped signal pulse and the TTD reference pulse are mixed in a nonlinear optical crystal producing a second harmonic field that carries the spatial image of the temporal shaped signal pulse. The time scaling of the system is set by the magnification of the anamorphic imaging system as well as the grating frequency and the time window of the system is set by the size of the grating aperture. Our experimental results show a time window of 20 ps.

The new pulse correlation technique is shown schematically in Fig. 7. It employs a grating at the entrance of the anamorphic imaging system, introducing a tilt in the pulse front with respect to the wave front. This tilt of the pulse front causes a Transverse Time Delay (TTD) across the spatial extent of the pulse. Next, the shaped signal pulse and the TTD reference pulse are mixed in a nonlinear optical crystal at the image plane of the anamorphic imaging system, producing a second harmonic field see Fig. Our technique allows for decoupling of the time

delay from the propagation direction, permitting us to select the angle between the intersecting pulses in the vertical direction (see angle  $\phi$  in Fig. 7) to achieve the phase matching conditions for the best efficiency. The time scaling of the system is set independently by adjusting the pulse front tilt angle  $\theta$  in the orthogonal, horizontal direction.

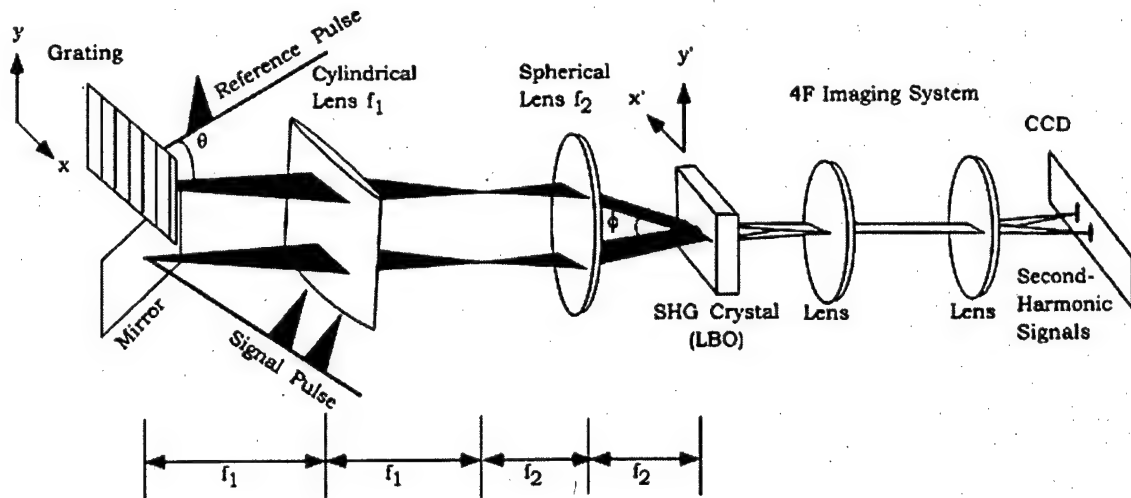


Fig. 7 Schematic diagram of the experimental TTD time domain pulse correlation system: the tilted time front is in the x-direction, enabling the use of the y-direction for optimizing the phase matching conditions of the SHG process

The experimental setup is schematically shown in Fig. 7. We use a mode-locked Ti:Sapphire laser producing 200fs pulses with center wavelength of  $\lambda = 920$  nm. The laser output beam is collimated and magnified before entering the pulse correlation system to ensure that the spatial intensity profile of the pulse is uniform across the crystal aperture. The optical pulse entering into the pulse correlation system is split into two beams by a beam splitter; one beam is used to provide a reference pulse and the other a signal pulse. The latter can be introduced into a pulse-shaping device to generate a pulse sequence employing spectral domain filtering of the initial pulse.

The reference pulse impinges on a metallic blazed grating of 600 lines/mm. The anamorphic imaging system consists of a cylindrical lens and a spherical lens. The two beams are imaged in the horizontal direction, x, and focused in the vertical direction, y, at the back focal plane of the second lens. The signal and the reference beams are parallel to each other with a vertical separation to introduce an angle of the intersection of two pulse beams in the focal plane of the second lens. This angle is optimized to satisfy the phase matching condition in the SHG crystal. A delay line is inserted in the path of the signal beam to control the overlap between the signal and reference pulses in time and space in the volume of the nonlinear optical crystal. A nonlinear optical crystal  $\text{LiB}_3\text{O}_5$  is placed in the image plane of the system. The crystal cut and the crystal orientation are designed to satisfy the type I phase-matching condition for non-collinear second-harmonic generation. With this setup, the generated second-harmonic field propagates in the vertical bisector direction, coinciding with the direction of the optical axis of the system. Background noise is spatially filtered, and a dichroic filter is placed in front of the CCD camera to block IR pulses.

We perform pulse imaging experiments with various shaped pulses obtained at the output of the pulse-shaping device. We prepare a sequence of pulses using this filter in the pulse shaper and then use our pulse correlation system to analyze this signal. The experimental results are shown in Fig. 8. The three pulses separated by 2.53 ps show excellent agreement with the calculated separation value of 2.50 ps (see Fig. 8 a). In our second cross-correlation experiment,

shown in Fig 8b, we use a 50/50 binary amplitude grating (i.e., a Ronchi grating) with a  $250\text{ }\mu\text{m}$  grating period as a spectral filter. Such a grating has the unique property that its Fraunhofer diffraction pattern does not have even-diffraction orders except for the  $0^{\text{th}}$  order. The obtained image of the sequence of the pulses does not show the even-order pulses. The three central pulses, corresponding to the -1, 0, and +1 orders, are separated by  $1.75\text{ ps}$  while the higher orders are separated by twice that distance. The separation of the central three pulses is consistent with the calculated value of  $1.69\text{ ps}$ .

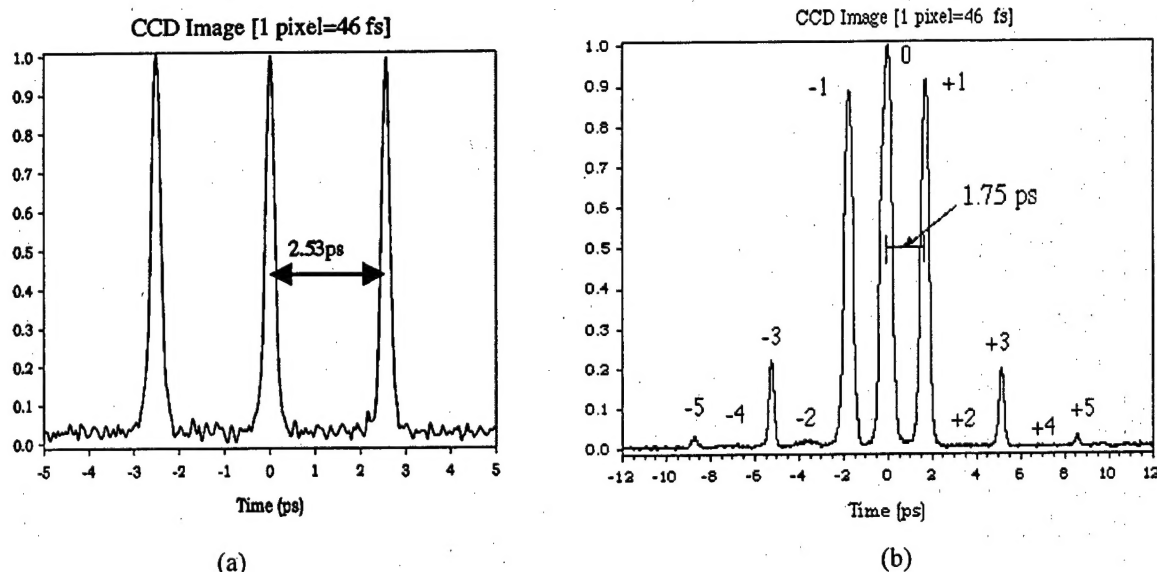


Fig.8 Shaped pulses obtained with the TTD pulse correlation system: A sequence of pulses (a) obtained using a pulse shaper with a phase spectral filter having 3 diffraction orders of equal amplitude, and (b) obtained using a pulse-shaper with a Ronchi grating spectral filter

## 5. Personnel Supported

Y. Fainman, PI, Professor  
P. C. Sun, co-PI, Assistant Research Scientist  
Danny Marom, Research Assistant  
Dmitriy. Panasenکو, Research Assistant  
Nathan Shou, Research Assistant  
Kaz Oba, Research Assistant  
Lijun Zhu, Research Assistant

## 6. Publications

D. Marom, P. C. Sun, Y. Fainman, "Analysis of spatio/temporal converters for all-optical communication links," *Appl. Opt.*, 37, 2858-2868, 1998.  
K. Oba, P. C. Sun, and Y. Fainman, "Nonvolatile photorefractive spectral holography," *Opt. Lett.*, 23, 915-917, 1998.  
Y. Mazurenko and Y. Fainman, "Cross talk of wavelength-multiplexed quasi-infinite holograms," *Opt. Lett.*, 23, 963-965, 1998.

D. M. Marom, D. Panasenکو, P. C. Sun, and Y. Fainman, "Spatial-temporal wave mixing for space-time conversion," *Opt. Lett.* **24**, 563-565(1999)

P. C. Sun, Y. Mazurenko, and Y. Fainman, "Space-time processing with photorefractive volume holography," *Proceedings of IEEE*, 1999, in press (invited paper)

K. Oba, P. C. Sun, Y. Mazurenko, and Y. Fainman, "Femtosecond single-shot correlation system: a time domain approach," *Applied Optics*, Vol. 38, no. 17, pp3810-3817, 1999

P. C. Sun, Y. Mazurenko, and Y. Fainman, "Space-time processing with photorefractive volume holography using femtosecond laser pulses," Ch. 15 in book *Photorefractive: Materials Properties and Applications*, eds. F. T. S. Yu and S. Yin, Academic Press, 1999 (in press)

Y. Fainman, P. C. Sun, Y. Mazurenko, D. Marom, and K. Oba, "Nonlinear spatio-temporal processing with femtosecond laser pulses," NATO Science Series on *Unconventional Optical Elements for Information Storage, Processing, and Communication*, ed. N. A. Vianos, Kluwer academic publishers, Netherlands, 1999 (in press)

M. Marom, D. Panasenکو, R. Rokitski, P.-C. Sun, and Y. Fainman, "Instantaneous processing of ultrafast waveforms by wave mixing spectrally decomposed waves," accepted for publication in special issue of *Opt. and Photon. News*, summarizing optics activity in 1999 (in press).

D. M. Marom, D. Panasenکو, R. Rokitski, P.-C. Sun, and Y. Fainman, "Time reversal of ultrafast waveforms by wave mixing spectrally decomposed waves," accepted for publication in *Opt. Lett.* (in press)

## **7. Interactions/transitions**

### **a. Meetings, Conferences, Seminars, Proceedings**

D. Marom, P. C. Sun, Y. Fainman, "Communication with ultrashort pulses and parallel-to-serial and serial-to-parallel converters," *Proc. IEEE/LEOS*, v. 1, p. 32-33, 1997, presented at the 10-th Annual Meeting of IEEE/LEOS, 1997.

Y. Fainman, "Optical interconnect systems for communications and computing," *Proc. IEEE/LEOS*, v. 2, p. 343-344, 1997, presented at the 10-th Annual Meeting of IEEE/LEOS, 1997 (invited).

K. Oba, P. C. Sun, Y. Fainman, "Nonvolatile photorefractive spectral holography for time-domain storage of femtosecond pulses," *CLEO'97*, v. 11, 213-214, Baltimore, 1997.

Y. Fainman, "Space-time Information Processing with femtosecond Laser Pulses," presented at the International conference on Optics in Computing, June 17-20, 1998, Brugge, Belgium; *Proc. SPIE*, 3490, 258-261, 1998 (Invited paper).

D. Marom, K. Oba, P. C. Sun, Y. Mazurenko, and Y. Fainman, "Spatio-temporal Conversion, Storage, and Processing using Femtosecond Optical Pulses," presented at the SPIE 43-rd Annual Meeting, July 1998, San Diego, California; *Proc. SPIE*, 3470, 64-76, 1998 *Proceedings of the SPIE - The International Society for Optical Engineering*, 1998, vol.3470:64-76 (Invited paper).

K. Oba, X. Zhang, P. C. Sun, Y. Mazurenko and Y. Fainman, "Single shot femtosecond/picosecond autocorrelator using tilted pulse front," presented at the SPIE 43-rd Annual Meeting, July 1998, San Diego, California; *Proc. SPIE*, 3466, 1998.

Y. Fainman and P. C. Sun, "Spatio-Temporal storage and retrieval with femtosecond optical pulses," 1998 International Photonics Conference, December 15-18, 1998, National Taiwan University, Taipei, Taiwan (Invited)

D. M. Marom, P.-C. Sun, and Y. Fainman, "Analysis of time-to-space converter," OSA Annual Meeting, Baltimore, MD, Oct. 98

Y. Fainman, "Nonlinear spatio-temporal processing for coherent optical communications," presented at the 1998 OSA Annual Meeting, October 4-9, 1998, Baltimore Maryland (Invited).



D. M. Marom, L. B. Milstein, and Y. Fainman, "Hybrid optical code division multiple access/pulse position modulation technique with self-referencing," OSA Annual Meeting, Baltimore, MD, Oct.19 98.

D. M. Marom, D. Panasenکو, P.-C. Sun, and Y. Fainman, "Real-time spatial-temporal signal processing by wave-mixing with cascaded second-order nonlinearities," presented at the OSA topical meeting on Optics for Computing, Technical Digest, 161-163, Snowmass Village, CO, 13-16 April 1999.

M. Marom, D. Panasenکو, P.-C. Sun, and Y. Fainman, "Spatial-temporal pulse waveform synthesis by wave-mixing with cascaded second-order nonlinearities," presented in Conference on Lasers and Electro-optics 1999 (CLEO'99), Baltimore, MD, 23-28 May 1999 (invited)

Y. Fainman, P. C. Sun, Y. Mazurenکو, D. Marom, and K. Oba, "Nonlinear spatio-temporal processing with femtosecond laser pulses," presented at the NATO Workshop on "Unconventional Optical Elements for Information Storage, Processing, and Communication", Kiryat Anavim, Israel, October 19-22, 1999.

Y. Fainman, D. Marom, K. Oba, D. Panasenکو, Y. Mazurenکو, and P. C. Sun, "Nonlinear space-time information processing," presented at the Euro-American Workshop on Optoelectronic Information Processing, Colmar, France, May 31-June 2, 1999; also to appear in the Critical review of SPIE, Optoelectronic Information Processing, B. Javidy and P. Refregier, ed. 1999 (in press). (Invited)

M. Marom, D. Panasenکو, R. Rokitski, P.-C. Sun, and Y. Fainman, "Instantaneous time reversal of complex amplitude ultrafast waveforms," accepted for presentation at IEEE Lasers and Electro-Optics Society 1999 Annual Meeting.

Y. Fainman, D. M. Marom, K. Oba, D. Panasenکو, Y. T. Mazurenکو, and P. C. Sun, "Nonlinear Spatio-temporal Processing," accepted for presentation at IEEE Lasers and Electro-Optics Society 1999 Annual Meeting (invited).

#### **b. Consultative and advisory functions**

Y. Fainman "Real-time optical analog-to-digital (ROAD) converters," presented at the DARPA Workshop on A/D Converter Technology, Arlington, October 1997.

Y. Fainman, "Optics in computing and communications," presentation and participation on the pannel "Potential Roles of Ultrafast Optics in Communications and Information Processing" at the 10-th Annual Meeting of IEEE/LEOS, 1997.

Y. Fainman, P. C. Sun, Y. Mazurenکو, K. Oba, D. Marom, "Storage formats for ultrahigh speed communication and processing, presented at the AFOSR Workshop on Applications of Spectral Hole Burning, March 8-11, Montana State University, Bozman, Montana, 1998.

Y. Fainman, P. C. Sun, Y. Mazurenکو, K. Oba, D. Marom, "Nonlinear Spatio-temporal Wave Mixing and Applications", presented at the AFOSR Workshop on Applications of Spectral Hole Burning, March 8-10, Montana State University, Bozman, Montana, 1999.

#### **8. New discoveries:**

None

#### **9. Honors/Awards:**

None



AIR FORCE OFFICE OF SCIENTIFIC  
RESEARCH (AFOSR)  
NOTICE OF TRANSMITTAL TO DTIC. THIS  
TECHNICAL REPORT HAS BEEN REVIEWED  
AND IS APPROVED FOR PUBLIC RELEASE  
IWA AFR 190-12. DISTRIBUTION IS  
UNLIMITED  
YONNE MASON  
STINFO PROGRAM MANAGER